Quantum Electronics **51** (5) 393–399 (2021)

https://doi.org/10.1070/QEL17546

Mass spectrometry of volatile organic compounds ionised by laser plasma radiation

A.B. Bukharina, A.V. Pento, Ya.O. Simanovsky, S.M. Nikiforov

Abstract. **Vacuum UV radiation from laser-induced plasma is used to ionise volatile organic compounds (VOCs) released by living organisms during their mass spectrometric analysis at atmospheric pressure without sample preparation. It is shown that the probability of ionisation of organic compounds with different ionisation potentials and proton affinity at atmospheric pressure in the argon flow weakly depends on the compound parameters and can be $3.6 \times 10^{-5} - 1.4 \times 10^{-4}$. The VOC spectra of mouse and human biological fluids are obtained without sample preparation at room temperature of the sample. The possibility of using the proposed method for the diagnosis of pathological changes is demonstrated.**

Keywords: *mass spectrometry, laser plasma, volatile organic compounds.*

1. Introduction

Currently, high-tech devices as well as diagnostic and treatment methods based on the use of various physical phenomena are widely employed in medicine.

One of the challenges facing medicine today is the development of new and more effective means of diagnosing and assessing the risks of developing diseases. A significant trend in modern postgenomic medicine is the transition from the 'validity' approach, that is, the search for biomarkers uniquely associated with specific pathologies, to a probabilistic risk assessment based on the analysis of the entire available part of the human molecular profile. This approach requires the development of technologies capable of providing broadband scanning of the molecular composition of a biological sample, including organic substances with a low molecular weight [1]. Among various alternative solutions to this problem, the development of high-performance methods for analysing the complex of volatile organic compounds (VOCs) released by animals and humans seems promising.

VOCs contain information about the individual's condition that can be used for diagnostic purposes [2, 3]. The advantages of this approach are noninvasive analysis, as well as minimal time for its implementation and cost. However, when analysing VOCs of biological objects, it is important to use a method that excludes long-term sample preparation. The sample interaction with atmospheric air components at room temperature, the evaporation of the volatile components, the effect of microflora that decomposes the components of the analysed samples, the sample interaction with the input tract materials – all this leads to a change in the ratio and even the composition of the VOC components in the sample. Therefore, despite the presence of well-developed methods of analysis that combine mass spectrometry with gas chromatography and liquid chromatography and are used in medical practice [4, 5], methods are being developed that allow the analysis of biological samples 'as they are', without sample preparation. An example is the direct analysis in real time (DART) method, which uses a flow of metastable noble gas atoms to ionise organic compounds [6]. Another example is the desorption electrospray ionisation (DESI) method, in which a flow of ions formed as a result of electrospray deposition of special solutions is used to ionise chemical compounds [7]. Both of these approaches are implemented in commercially available devices that allow analysing samples without sample preparation. However, these methods have certain disadvantages, which, in particular, include the relatively low efficiency of ion formation and the limited class of compounds to be determined. In addition, these methods do not provide the necessary 'broadband' analysis.

An effective method of ionisation of organic compounds is the proton exchange reaction. These reactions are used in proton transfer mass spectrometry [8, 9], which is currently the most efficient method of VOC analysis. In this method, the proton-donating compound is the molecular ion H_3O^+, which is produced in a special chamber using, as a rule, a glow discharge. The development of this method is the technology of selected ion flow tube mass spectrometry (SIFT-MS) [10], based on the preliminary selection of reagent ions in a quadrupole filter.

The expansion of the range of ionised VOCs is possible due to the use, for example, of pulsed broadband UV radiation of laser-induced plasma, as we have shown earlier in works [11–13]. The proposed method of ionisation is called atmospheric pressure laser plasma ionisation (APLPI). Laser plasma generated by pulsed radiation is a source of vacuum UV radiation that can be used to ionise VOCs. Measurements (performed in work [14]) of the spectral characteristics of laser plasma radiation produced at the surface of a stainless steel target under the action of pulsed laser radiation with a wavelength of 1.064 μm, a pulse energy of 250 mJ and a power density of ~70 GW cm^{-2} have shown that during the first 4–5 ns the radiation spectrum of laser-induced plasma has no pronounced lines. The plasma radiation intensity rapidly decreased, and after 15–20 ns, the spectral lines of the target material atoms became visible and then dominated

A.B. Bukharina, A.V. Pento, Ya.O. Simanovsky, S.M. Nikiforov
Prokhorov General Physics Institute, Russian Academy of Sciences, ul. Vavilova 38, 119991 Moscow, Russia; e-mail: Ay15@mail.ru

Received 1 March 2021
Kvantovaya Elektronika **51** (5) 393–399 (2021)
Translated by M.A. Monastyrskiy

until the end of the observation interval, which was 250 ns from the time moment of exposure to the laser pulse. The plasma spectrum within the initial time interval can be approximated by the black body spectrum with a certain temperature. The correlation between the temperature obtained from the line spectra of the target material and the intensity of the structureless component of the spectrum allows us to estimate the temperature and, accordingly, the plasma radiation spectrum in the first few nanoseconds. The resulting temperature estimate is 5×10^4 K. At this temperature, more than half the black body radiation energy falls within the wavelength range of less than 100 nm (photon energy above 12 eV), which provides ionisation of molecules of almost any organic compound, atmospheric gases, water, and noble gas atoms. However, in the first works in this direction, the probability of ion formation in the mass spectrometer's ion source was not determined. In contrast to the frequently used detection threshold, this value characterises the physical process of ion formation and is not related to the parameters of the mass spectrometers used.

A common approach when using VOC analysis for identification of pathology is to compare the VOC spectra of sick and healthy individuals. Since this approach requires a significant amount of experimental data, the sensitivity and performance of the analysis method become key factors. The method we are developing allows us to perform analysis without sample preparation, with high sensitivity and in the shortest possible time.

The objectives of this work are to determine the probability of ionisation of organic compounds with various parameters in an ion source with laser plasma at atmospheric pressure, and to evaluate the capabilities of the APLPI method for detecting a complex of VOCs released from biological fluids of living organisms.

2. Experimental setup for mass spectral analysis of VOCs

A schematic of the experimental set up for mass spectrometric analysis of VOCs in biological fluids at atmospheric pressure with ionisation by laser plasma radiation is shown in Fig. 1.

A quadrupole-time-of-flight (QTOF) mass spectrometer (*1*) with the atmospheric pressure ion transfer interface provided a resolution of $m/\Delta m = 5000$ for $m/z = 609$ and a mass determination error of $\delta m = 2 \times 10^{-5} m$. A sealed ionisation chamber (*2*) was installed on the input flange of the mass spectrometer, inside which a metal target (*3*) was placed near the input hole of the mass analyser to generate laser plasma. The target was a stainless steel disk and rotated at a frequency of ~30 rpm to reduce the effect of the target material erosion on the formation of laser-induced plasma. A pure carrier gas (argon 99.995) was blown through the ionisation chamber.

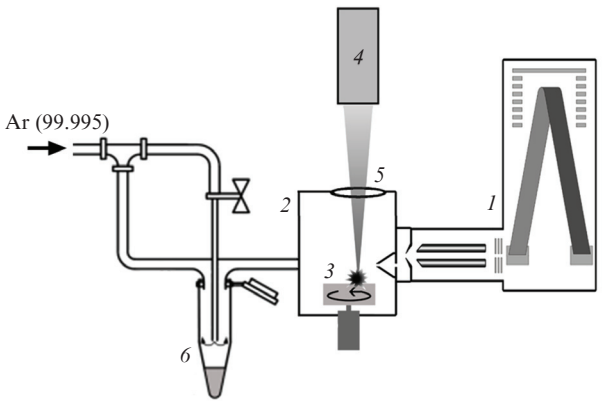

Figure 1. Schematic of a laser mass spectrometer for VOC analysis: (*1*) time-of-flight mass analyser; (*2*) ionisation chamber; (*3*) rotating metal target for the generation of laser-induced plasma; (*4*) Nd:YAG laser; (*5*) focusing lens; (*6*) microcentrifuge test-tube with a sample.

Laser-induced plasma was generated on the surface of a rotating target by pulsed radiation (wavelength 1.06 μm) of an RL-03/355 diode-pumped Nd:YAG laser (Russia, Moscow, ELS-94 Ltd) (*4*). The laser pulse repetition rate was 300 Hz, the pulse duration was 0.5 ns, and the pulse energy was 250 mJ. Using a lens (*5*) with a focal length of 5 cm, laser radiation was focused on the target surface into a spot with a diameter of ~30 μm, which provided a radiation power density of ~70 GW cm^{-2}. Plasma was formed at a distance of ~2 mm from the device axis and ~3 mm from the inlet.

The analysed sample of biological fluid was placed in a microcentrifuge test-tube *6*, which was installed on a sealed pneumatic connector of the ionisation chamber's inlet line and blown through with a flow of pure argon. The VOC samples were transferred by the carrier gas flow into the ionisation chamber, where they were ionised. The carrier gas flow was split so that 90% of the flow went directly into the chamber and 10% passed through the test-tube with a sample. To prevent the ambient atmospheric air from entering the chamber when changing the test-tubes with samples, an excess pressure of 30 Torr was maintained in the chamber. The carrier gas flow rate (~6 cm^3 s^{-1}) approximately corresponded to the sampling rate of the gaseous sample by the mass analyser.

To measure the ionisation probability, vapours of volatile substances were fed into the chamber from a balloon through a quartz capillary with an internal diameter of 30 μm and a length of 60 cm. The substance flow was controlled by changing its concentration in the balloon and changing the pressure drop between the balloon and ionisation chamber. The flow was calculated using the well-known Poiseuille equation for viscous gas flow through a thin cylindrical tube.

The probability of ionisation of an organic compound in an experiment is defined as the ratio of the ion flux of the compound to the flux of its neutral molecules. However, the ion flux in measurements with a mass spectrometer is recorded by a mass analyser, the ion transmission efficience of which is unknown. Therefore, in most studies dedicated to the mass spectrometric determination of VOCs, it is not the ionisation probability that is determined, but the detection threshold of a particular compound, which relates more to the instrument used than to the physical process of ion formation.

In our device, ions of the analysed compounds and of surrounding gas from the area with atmospheric pressure, passing through the transport system of the mass analyser, overcome four stages of differential pumping until they reach the time-of-flight section of the mass analyser. In the course of transportation, some of the ions are neutralised on the metal electrodes of the ion-optical part of the transport system or leave the region of stable transportation and, thus, do not contribute to the recorded ion signal.

To determine the mass analyser transmittance, we measured the current of positive ions at the transport system input (the measurement scheme is shown in Fig. 2a) and the corresponding current at the ion detector of the time-of-flight mass spectrometer. Positive and negative ions formed under

the action of laser plasma inside an ionisation chamber (*1*) enter through an inlet aperture with a diameter of 0.3 mm into a metal intermediate chamber (*2*) evacuated to a pressure of 2 Torr, and then through a skimmer (*3*), into a transport quadrupole chamber (*4*) evacuated to a pressure of 5×10^{-3} Torr. The current of ions neutralised on the skimmer was measured with a Keithley 6485 picoammeter (*5*). Ethanol was used as an analyte, the vapours of which were fed into the ionisation chamber through a capillary (*6*), and argon was used as a carrier gas. In the mass spectrum recording regime, the skimmer potential was 30 V lower than the potential of the intermediate chamber, which created preferable conditions for the transport of positive ions. An increase in the potential difference to a value exceeding 35 V leads to the saturation of the recorded current dependence on the potential difference due to the neutralisation on the skimmer of all incoming ions. The measured saturation current I^+ can serve as an estimate of the number of positive ions entering the mass analyser inlet, without taking into account the loss of ions at the chamber input. The flux N of ions neutralised on the skimmer is determined from the simple relation $N = I^+/e$, where $e = 1.6 \times 10^{-19}$ C is the electron charge. The experimentally recorded current $I^+ = 25$ pA corresponds to the ion flux $N = 1.6 \times 10^8$ s^{-1}.

Under the same conditions in the ionisation chamber, the ion detector of the time-of-flight mass spectrometer records the characteristic mass spectrum of ethanol (Fig. 2b) at a total ion current with an amplitude of 8×10^5 ADC counts per second, which, with an average amplitude of the single-ion pulse of the detector equal to 5 ADC counts, corresponds to an ion flux of 1.6×10^5 s^{-1}. The ion transport efficiency, defined as the ratio of the output and input ion fluxes, was 10^{-3}.

3. Results

3.1. VOC ionisation by laser-induced plasma radiation

Figure 3a shows the mass spectrum of ions produced in pure argon (99.995) at atmospheric pressure and exposure to pulsed UV radiation from laser plasma. The dominant peaks in the analyte absence are the peaks of the $[H_2O + H_3O]^+$ and $[(H_2O)_2 + H_3O]^+$ ions, the source of which is obviously the H_2O^+. ion. In addition to these peaks, some peaks of significantly lower intensity are observed in the spectrum, which are of interest for understanding the ion formation process. These are N_2^+, O_2^+ and Ar^+ ions, as well as protonated N_2H^+, O_2H^+, and ArH^+ ions. Oxygen and nitrogen are present in argon as impurities with a concentration of tens of ppm. The forma-

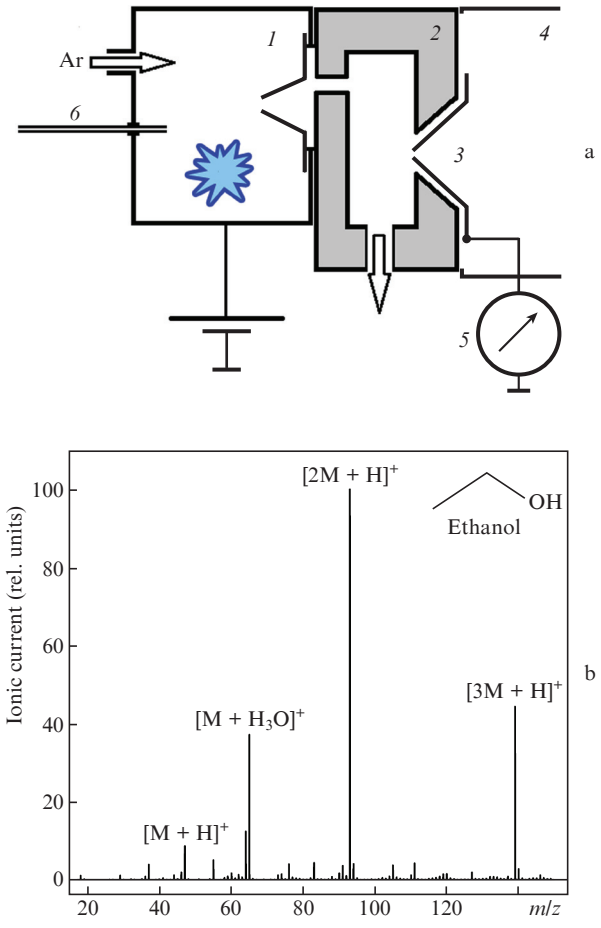

Figure 2. (a) Scheme for measuring the current of ions entering the transport system of the mass analyser and (b) the mass spectrum of ethanol vapours:
(*1*) ionisation chamber; (*2*) intermediate chamber; (*3*) skimmer; (*4*) transport quadrupole chamber; (*5*) electrometer; (*6*) capillary for introducing the analyte.

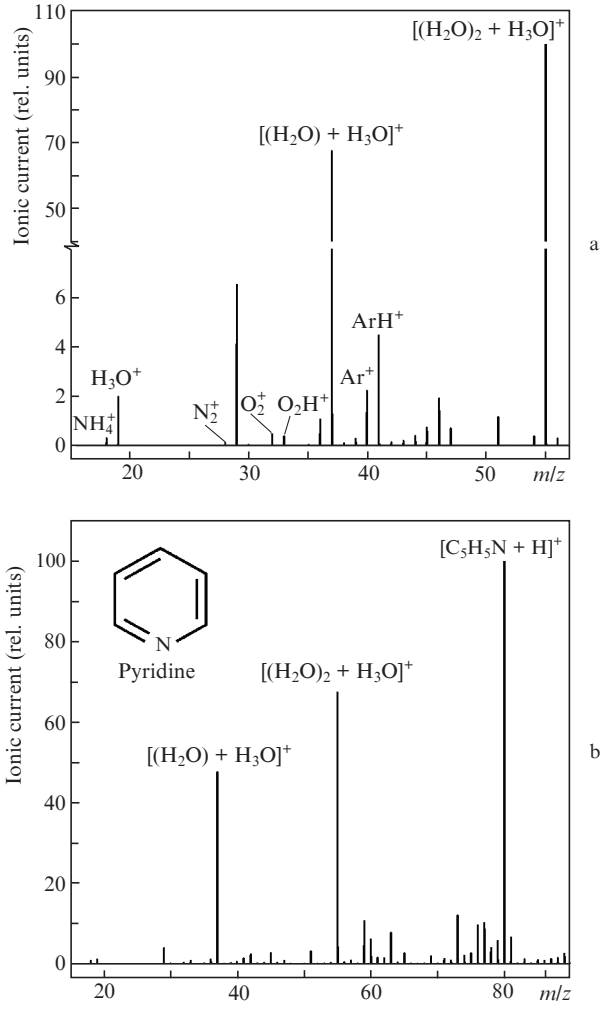

Figure 3. Mass spectra of ions (a) in pure argon and (b) in the case of injection pyridine with a flow of 1.25×10^{11} mol s^{-1}.

tion of molecular nitrogen and oxygen ions and argon ion is associated with the photoionisation of the corresponding substances by hard UV radiation. The spectrum of UV radiation propagating in the ionisation chamber is limited by the wavelength of the argon absorption edge (80 nm, quantum energy 15.45 eV); therefore, photoionisation of oxygen, nitrogen, and water is possible.

Figure 3b shows the mass spectrum obtained by injecting pyridine vapours (C_6H_5N, 79 amu) into the ionisation chamber with a flow of 1.25×10^{11} mol s^{-1}. Since all the gas supplied to the chamber enters the mass spectrometer, this value corresponds to the input flow of neutral molecules, and its ratio to the argon flow gives the analyte concentration in the ionisation chamber. At an argon flow of 7 cm^3 s^{-1}, it is $1.25 \times 10^{11}/ (7 \times 2.7 \times 10^{19}) = 660$ ppt.

One can see from Fig. 3b that the protonated pyridine ion is recorded in the mass spectrum, i.e., the analyte ion is formed due to the proton transfer reaction. The concentration of water vapour in pure argon is at least three orders of magnitude higher than the concentration of recorded analytes. Pulsed UV radiation with a quantum energy of more than 12.6 eV causes the formation of H_2O^+ ions with a concentration exceeding the concentration of analyte ions by several orders of magnitude. This is also due to the fact that the photoionisation cross sections of molecular compounds are quite close. Possible reactions involving water molecules and M analyte can be written as follows:

$$M + h\nu = M^+ + e, \quad (1)$$

$$H_2O + h\nu = H_2O^+, \quad (2)$$

$$H_2O^+ + H_2O = H_3O^+ + OH, \quad (3)$$

$$M + H_2O^+ = MH^+ + OH, \quad (4)$$

$$M + H_3O^+ = MH^+ + H_2O. \quad (5)$$

The proton transfer reaction is not the only channel for the formation of analyte ions. As shown in work [14], possible channels are photoionisation, electrophilic addition reaction, and oxidation with postionisation. Photoionisation (1) is observed mainly for aromatic compounds – aniline, benzene, and toluene. However, for most compounds, the main channel is the formation of a protonated MH^+ ion due to proton exchange reactions (4) and (5). In contrast to proton transfer mass spectrometry, in our case, the proton source is not only H_3O^+, but also H_2O^+ and OH^+. The OH radical has a proton affinity that is lower than that of H_2O (593 and 691 kJ mol^{-1}, respectively [15]), which makes it possible to expand the class of compounds ionised by this method.

Broadband UV radiation with a wavelength of less than 239 nm can cause photodissociation of a water molecule, as it occurs in the Earth's atmosphere [16]. In the presence of vacuum UV radiation, this creates two more types of proton-donating agents – OH^+ and H^+ with ionisation potentials of 13 and 13.6 eV, respectively:

$$H_2O + h\nu = OH + H, \quad (6)$$

$$OH + h\nu = OH^+ + e, \quad (7)$$

$$H + h\nu = H^+ + e, \quad (8)$$

$$M + OH^+ = MH^+ + O, \quad (9)$$

$$M + H^+ = MH^+. \quad (10)$$

The proton affinity for an oxygen atom is 485 kJ mol^{-1} [17]; therefore, the OH^+ radical ion is the most efficient proton-donating compound. The presence of free H^+ ions may explain the appearance of N_2H^+, O_2H^+, and ArH^+ ions. The proton affinity for these substances is 494, 421, and 369 kJ mol^{-1}, respectively [17]. Finally, when using inert gases, the analyte ionisation is possible due to the Penning effect [18]. However, for argon, this channel becomes inefficient, since the energy of the metastable $^3P_2$ level (11.6 eV) is less than the ionisation potential of the water molecule (12.6 eV).

In proton transfer mass spectrometry and SIFT-MS technology, the formation of reagent ions occurs in a special chamber, while the process of analyte ionisation itself takes place in a drift tube. These processes are separated in space. Photoionisation and subsequent formation of proton-donating compounds using laser plasma radiation occur directly in the gas containing the compounds to be detected, which allows several reactions to occur simultaneously, leading to the formation of target ions. The result should be the equalisation of the ion formation efficiency for compounds with different proton affinities, which is necessary for the analysis of a wide range of VOCs released by living organisms.

3.2. Determination of the probability of the formation of organic compound ions in ionisation by laser plasma radiation

To determine the formation probability of ions of various organic compounds at atmospheric pressure of argon, vapours of substances with a strictly controlled flow rate in the range 10^{10}–10^{11} mol s^{-1} were fed into the ion source chamber. Table 1 shows the device sensitivity defined as the ratio of the flux of neutral molecules to the flux of detected ions at the mass spectrometer output, and also the probability of the formation of an ion of a particular compound obtained as a product of the mass analyser's sensitivity and transmittance.

It can be seen from Table 1 that the probability of ion formation for compounds of different classes with different

Table 1. Mass spectrometry of volatile organic compounds in ionisation by laser plasma radiation.

Substance	Sensitivity/ion molecule^{-1}	Proton affinity/kJ mol^{-1}	Ionisation potential/eV	Ion formation probability
Ethanol	7.2×10^{-9}	776.4 [15]	10.5 [17]	7.2×10^{-6}
Hexane	4.6×10^{-9}	673 [19]	10 [17]	4.6×10^{-6}
Pyridine	2.8×10^{-8}	930 [15]	9.26 [17]	2.8×10^{-5}
D-limonene	1.7×10^{-8}	842 [20]	8.3 [21]	1.7×10^{-5}
Acetone	5.0×10^{-8}	812 [15]	9.7 [17]	5.0×10^{-5}

ionisation potentials and proton affinities differ by less than 10 times. In this case, the probability of ion formation reaches 1.7×10^{-5}, which is comparable to the probability of molecule ionisation by electron impact. However, ionisation by laser plasma radiation is, in contrast to electron impact ionisation, a 'soft' ionisation method, which in most cases does not lead to fragmentation of organic molecules. The combination of high ionisation probability and minimal fragmentation makes it possible to use the developed method for VOC analysis.

3.3. VOC analysis of mouse and human biological fluids

The aim of our experiments with biological fluids was to find regimes in which it would be possible to analyse VOCs released by biological fluids without sample preparation at room temperature of the sample. Four groups of biological fluid samples were used in the experiments: urine of mice, and also urine, saliva, and bile of a human. All samples were analysed without sample preparation, in the 'as they are' state.

Figure 4 shows the mass spectra of urine of the same mouse from a group of mice, obtained in an experiment on the development of a cancerous tumour. The first mass spectrum was recorded before the experiment's start; the second, a day after the inoculation of cancer cells; and finally, the third, at the stage of tumour development. It can be seen that, as the disease develops, pronounced changes are observed in the mass spectra. Changes in mass spectra are associated with changes in the body, its reactions to trauma, and tumour development [22]. The reproducibility of the mass spectra for the same sample was checked repeatedly. Experiments have shown that the root-mean-square deviation for both the total ion current and individual spectral peaks does not exceed 10%. The intensities of individual spectral peaks for the same sample were always reproducible.

Figure 5 shows the spectra of healthy human urine and human urine with a high concentration of acetone. There is also an identification of the main peaks. The formation of protonated dimers and adducts with ammonium indicates a high concentration of acetone in the urine. This phenomenon is known as acetonuria and is sometimes a sign of the decease.

Figure 6 displays the VOC mass spectra of bile samples obtained from noninflamed and inflamed gallbladders in the course of surgery. As in previous experiments, significant differences are observed in the mass spectra, namely, in the composition of the compounds and the amplitude of the total ion current.

Figure 7 demonstrates the mass spectra of saliva samples from the parotid salivary gland taken from five healthy patients. Taking a sample from the salivary glands allows one to obtain a clean sample, excluding the effect of nondiagnostic factors, i.e. traces of food, smoking, etc. The study was also conducted without sample preparation at room temperature of the sample. It can be seen that the mass spectra of all saliva samples taken from different patients contain approximately the same set of peaks, which is due to the similar composition and the same functional purpose of the studied samples. In this case, the differences may be due to both the individual characteristics of the patients and the presence of pathological changes.

Most often, a sign of the disease can be a change in the ratios of compound concentrations within a set of compounds in a sample of biological fluid, the number of which can reach several hundred [3]. In this case, it is impossible to isolate a specific marker compound in the sample, and classical statistical approaches and chemometric methods of data processing can be used to decide whether a particular sample belongs to groups with specific pathological changes or with their absence. Figure 8 presents the results of processing the mass spectra of the urine of healthy and cancer-infected mice using the principal component analysis, obtained earlier in our experiments [12, 13]. This method was used to process mass spectra in the range of 15–300 amu without distinguishing individual regions. It has been shown that this approach allows separating the mass spectra belonging to healthy and sick animals. The principal component analysis makes it possible to represent mass spectra in a new space of smaller dimension, i.e., in our case, each point in the space of the first two principal components (PC1 and PC2) corresponds to a single mass spectrum. This is a common approach to processing multidimensional data, including mass spectra, when it is not necessary to find any specific compounds being a marker of the disease, and it suffices to show the similarity or differ-

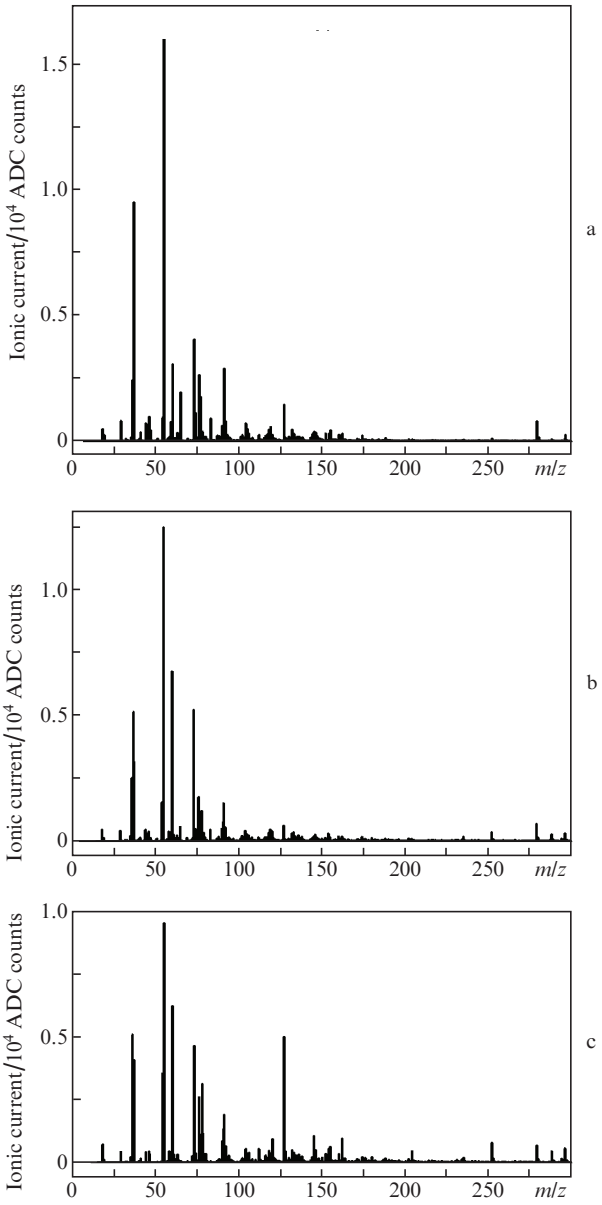

Figure 4. Mass spectra of urine samples taken from a mouse (a) before the experiment, (b) on the first day after inoculation, and (c) at the stage of tumour development.

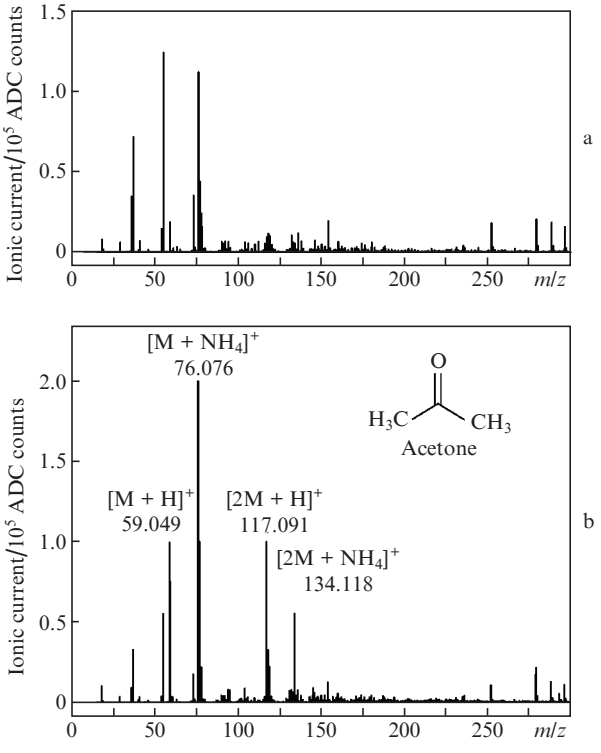

Figure 5. Mass spectra of urine of (a) a healthy individual and (b) human urine with a high concentration of acetone. In Fig. 5b, the letter M denotes an acetone molecule.

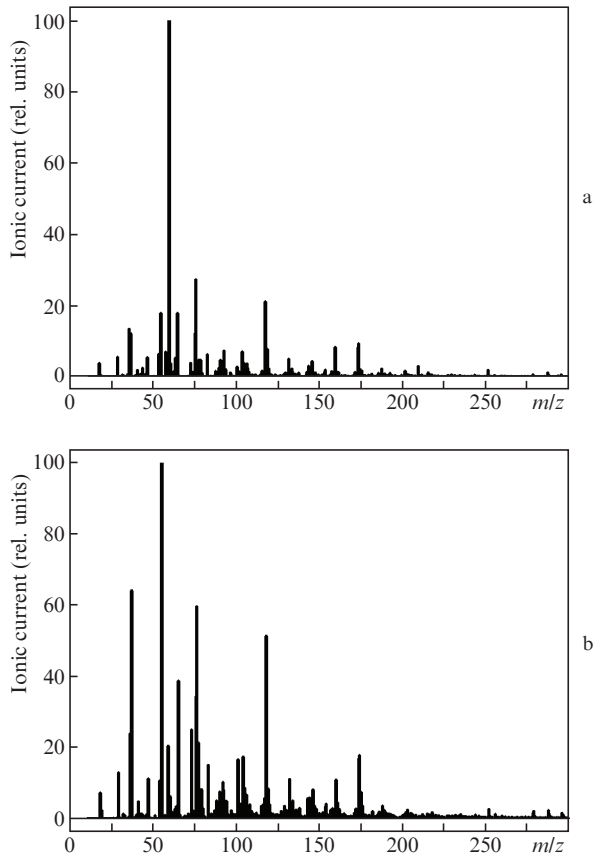

Figure 6. Mass spectra of bile of (a) healthy and (b) inflamed gallbladders.

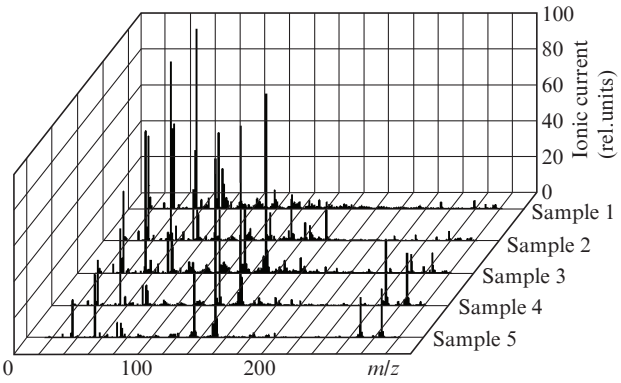

Figure 7. Mass spectra of human saliva samples taken from five patients from the parotid salivary gland.

ence of samples characterised by the distance in the space of principal components. Figure 8 clearly shows the grouping of the spectra of samples taken from mice infected with hepatocarcinoma and the spectra of samples taken from healthy mice.

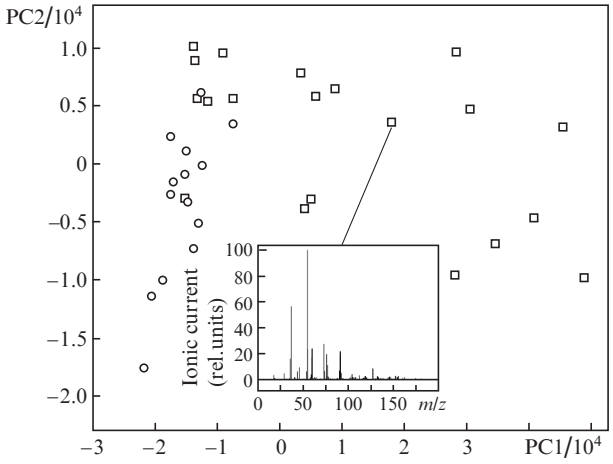

Figure 8. Results of processing of mass spectra of urine samples by the principal component method, the samples being taken from cancer-infected mice (circles) and intact mice (squares).

4. Conclusions

The method of ionisation of organic compounds by laser plasma radiation provides a high probability of the formation of protonated ions of organic compounds during ionisation in the argon flow at atmospheric pressure. The obtained values of the ionisation probability for compounds of various classes are in the range 7.2×10^{-6}–1.7×10^{-5} and correspond to a low VOC detection threshold. An important result is a relatively small difference in the ionisation probabilities for compounds with different values of the ionisation potential and proton affinity. This allows us to apply this method to the analysis of VOCs of living organisms, which are a complex mixture of organic compounds. Thanks to the sensitivity attained in our experiments, it is possible to analyse VOCs of biological fluids without sample preparation at room temperature of the sample. This makes it possible to significantly reduce the analysis time of a single sample. The full cycle of

obtaining mass spectra of a sample in our experiments takes ~1 min, whereas for chromatographic methods the required time reaches tens of minutes.

A common problem in the mass spectrometric analysis of VOCs of living organisms is a large scatter in the parameters of the mass spectra of samples taken from different individuals, formally combined into a single group based the presence or absence of pathology. Nevertheless, the use of the principal component analysis and, in the future, various machine learning methods provides a possibility of dividing healthy and sick individuals into groups, as shown in Fig. 8. In this approach, the mass spectrum is considered as a kind of 'an image', which is a single whole and does not require a detailed interpretation of each peak of the mass spectrum.

References

1. Lisitsa A.V., Ponomarenko E.A., Lokhov P.G., Archakov A.I. *Vestn. Ross. Akad. Med. Nauk*, **71**, 255 (2016).
2. Broza Y.Y., Mochalski P., Ruzsanyi V., Amann A., Haick H. *Angew. Chem. Int. Ed.*, **54**, 11036 (2015).
3. Amann A., de Lacy Costello B., Miekisch W., Schubert J., Buszewski B., Pleil J., Ratcliffe N., Risby T. *J. Breath Res.*, **8**, 034001 (2014).
4. Nair H., Clarke W. (Eds) *Mass Spectrometry for the Clinical Laboratory* (Academic Press, 2016).
5. French D. *Adv. Clin. Chem.*, **79**, 153 (2017).
6. Cody R.B., Laramée J.A., Nilles J.M., Durst H.D. *JEOL News*, **40**, 8 (2005).
7. Takats Z., Wiseman J.M., Gologan B., Cooks R.G. *Science*, **306**, 471 (2004).
8. Hansel A., Jordan A., Holzinger R., Prazeller P., Vogel W., Lindinger W. *Int. J. Mass Spectrom. Ion Processes*, **149**, 609 (1995).
9. Blake R.S., Monks P.S., Ellis A.M. *Chem. Rev.*, **109**, 861 (2009).
10. Smith D., Španěl P. *Mass Spectrom. Rev.*, **24**, 661 (2005).
11. Pento A.V., Nikiforov S.M., Simanovsky Ya.O., Grechnikov A.A., Alimpiev S.S. *Quantum Electron.*, **43**, 55 (2013) [*Kvantovaya Elektron.*, **43**, 55 (2013)].
12. Bukharina A., Pento A., Nikiforov S., Alimpiev S., Simanovsky Y., Grechnikov A. *Proc. 2018 Int. Conf. Laser Optics (ICLO)* (St. Petersburg, IEEE, 2018) p. 469. DOI: 10.1109/LO.2018.8435435.
13. Bukharina A.B., Kochevalina M.Y., Pento A.V., Simanovsky Y.O., Rodionova E.I., Nikiforov S.M. *Proc. 2020 Int. Conf. Laser Optics (ICLO)* (St. Petersburg, IEEE, 2020) p. 1. DOI: 10.1109/ICLO48556.2020.9285453.
14. Pento A.V., Bukharina A.B., Nikiforov S.M., Simanovsky Y.O., Sartakov B.G., Ablizen R.S., Fabelinsky V.I., Smirnov V.V., Grechnikov A.A. *Int. J. Mass Spectrom.*, **461**, 116498 (2021).
15. Hunter E.P., Lias S.G. *J. Phys. Chem. Ref. Data*, **27** (3), 413 (1998).
16. Brinkmann R.T. *J. Geophys. Res.*, **74**, 5355 (1969).
17. Lias S.G., in *NIST Chemistry WebBook – NIST Standard Reference Data-base Number 69* (Gaithersburg, MD, NIST, 2020) (retrieved 13.02.2020).
18. Smirnov B.M. *Sov. Phys. Usp.*, **24**, 251 (1981) [*Usp. Fiz. Nauk*, **133**, 569 (1981)].
19. Wroblewski T., Ziemczonek L., Szerement K., Karwasz G. *Czech. J. Phys.*, **56**, B1110 (2006).
20. Fernandez M.T., Williams C., Mason R.S., Costa Cabral B.J. *Faraday Trans.*, **94**, 1427 (1998).
21. Harris D., McKinnon S., Boyd R.K. *Org. Mass Spectrom.*, **14**, 265 (1979).
22. Schmidt K., Podmore I. https://downloads.hindawi.com/archive/2015/981458.pdf.